Epigenetic Remodeling in an IMR-32 Cell Line and Transgenic Mouse Model of

Alzheimer's Disease

Matthew Baker

A Senior Thesis submitted in partial fulfillment
of the requirements for graduation
in the Honors Program
Liberty University
Spring 2014

Acceptance of Senior Honors Thesis

This Senior Honors Thesis is accepted in partial
fulfillment of the requirements for graduation from the
Honors Program of Liberty University.

_____
Gary Isaacs, Ph.D.
Thesis Chair

_____
Mark Blais, D.P.M.
Committee Member

_____
Harvey Hartman, Th.D.
Committee Member

_____
Brenda Ayres, Ph.D.
Honors Director

_____
Date

Abstract

The pathological features of Alzheimer's disease (AD) have been researched and documented extensively, however the causes of these features are still unknown. The following studies sought to determine if epigenetic methylation alterations contribute to AD. Two studies were sequentially carried out, first using an IMR-32 model and then using a transgenic mouse model overexpressing beta-amyloid. A few assay and confirmation methods were carried out to determine the promoter regions in disease state models undergoing drastic change, and the genes linked to these promoter regions were analyzed to determine significant gene ontology being altered by this epigenetic modification. This data was further assessed in the transgenic mouse study by determining expression levels and transcription factor enrichment in the genes experiencing significant promoter methylation alterations. Both studies provided data supporting the idea that epigenetic methylation alterations are linked to genes having ontological functions associated with AD pathology. This conclusion supports the theory that epigenetics contributes to the development of AD.

Acknowledgements

Table of Contents

Introduction

Alzheimer's Disease

Alzheimer's disease (AD) is characterized by terminal tissue damage due to two main pathological findings: beta amyloid plaques and neurofibrillary tangles. Amyloid beta plaques (Aβ) are insoluble aggregates that develop due to overproduction of amyloid beta peptides, which ultimately leads to neuronal degeneration [1 Selkoe, 1991 #2]. Neurofibrillary tangles (NFTs) are the result of abnormal phosphorylation of the protein tau [2]. Tau is a microtubule-associated protein that is designed to help in the promotion and stabilization of microtubules to allow for proper axonal transport in neurons. The pathological phosphorylation of tau seen in AD inhibits it from supporting these necessary cellular functions and inversely causes neuronal cytoskeletal disassembly [3, 4]. These pathological findings have provided insight into what causes neurodegeneration to take place, however the causes of these characteristics and others seen in AD remain obscure.

Epigenetics

Evidence from past research seems to describe an epigenetic element to the development of AD. Epigenetics is defined as alterations in the transcription of an organism's genome due to factors that are outside the DNA sequence. In other words, epigenetics turns gene expression on and off to help in the development and life cycle of an organism. There are several types of epigenetic modifications that work to alter genomic transcription including histone acetylation, nucleosome placement, and DNA methylation, the last of which will be investigated extensively throughout this study.

DNA methylation is when a methyl (CH_3) group is chemically attached to the fifth carbon of a cytosine by enzymes known as DNA methyltransferases [5]. DNA methylation specifically targets the cytosine of the 5'-CpG-3' dinucleotide, which have been determined to be present in high volume in 40% of human gene promoter regions [6]. These 5'-CpG-3' rich promoter regions are known as CpG islands and these promoter regions characteristically contain low levels of DNA methylation [6]. Epigenetic methylation can impact genomic transcription through different mechanisms. First, the presence of methylation can prevent transcription factors from being able to bind to the promoter region of a gene, therefore inhibiting transcription. This mechanism is seen in transcriptional repression of the Foxp3 gene by DNA methylation in the promoter region [7]. Another mechanism is through promoting the binding of transcriptional repressors, which also inhibit transcription. For example, CpG methylation is required for the MeCP2 repressor protein to bind DNA and inhibit transcription [8]. The third mechanism by which methylation can inhibit transcription is through blocking progression of RNA polymerases [8]. Due to these consequences being the most prominent effect of DNA methylation, this epigenetic marker has been associated to transcriptional repression and gene silencing [9]. Nonetheless, exceptions are to be expected [10].

Epigenetics and Disease

Alterations in epigenetic markers and therefore genomic transcription is biologically normal throughout the life cycle of an organism due to different gene products being needed at different times [11]. However, past research has proven that epigenetic alterations are also involved in the development of disease states such as

cancer and syndromes linked to mental retardation [5]. Disease linked epigenetic

alterations have been found to yield hypomethylated and hypermethylated promoter

regions, although the prior is more typical of overall genomic alterations [12, 13]. For

example, cancer occurs when cells reproduce uncontrollably and avoid programmed cell

death [14]. Abnormal epigenetic methylation leads to this pathological state due to its

transcriptional impact on oncogenes and tumor suppressor genes. Oncogenes are genes

that signal the cell to reproduce constantly. Therefore, when the promoter region of these

genes is hypomethylated, transcription is not repressed through one of the mechanisms

described previously, leading to increased expression causing the cell to constantly

proliferate [15]. Hypermethylation has been found in the promoter region of tumor

suppressor genes, leading to decreased expression of gene products that keep dangerous

cells from becoming cancerous [16]. This substantiates the fact that the relationship

between alterations in the epigenetic methylation of promoter regions of the genome

deserve and disease development deserve substantial research. It is important to note that

global hypomethylation is seen in disease states due to this allowing for proliferation of

cells, as opposed to hypermethylation which causes gene silencing that would ultimately

lead to cell and organismal death if the genome was becoming globally hypermethylated.

Epigenetics and Alzheimer's Disease

Several factors contribute to the theory that epigenetic alterations, such as DNA

methylation, play a role in the development of AD. First, over 90% of AD cases are late

onset and appear to be sporadic, meaning that no genetic cause has been determined [17].

To expound on this factor, a non-Mendelian mode of acquiring AD is proposed due to the

fact that twin studies looking at the development of AD show differing results [18-20].

These studies suggest that DNA sequence alone does not lead to AD development. Second, research describes a parent-of-origin effect in AD, meaning that several genomic regions are passed down from the mother to affected individuals [21]. The most common method by which parent-of-origin effects are produced is mediated by DNA methylation, the focus of this study [22]. This environmental contribution, the maternal germ line, follows the mechanism of an epigenetic impact because it is outside the genetic code of an individual [23]. Third, mouse and human studies provide evidence that DNA methylation is altered between affected and control counterparts on a genomic level in DNA obtained from regions of the brain affected by AD [24]. While there were significant changes in diseased parts of the brain, methylation levels from unaffected regions of the brain remained unchanged between the affected and control counterparts. This specificity appears to be direct evidence that DNA methylation is involved in AD pathology. A fourth factor providing evidence for an epigenetic link to AD development is the fact that several genes that have been linked to AD pathology, such as APP, β-APP cleaving enzyme, and neprylisin, are transcriptionally regulated by DNA methylation in their promoter regions [25, 26]. Interestingly, although global hypomethylation is linked to AD, the neprylisin promoter is actually hypermethylated leading to its transcriptional silencing [26, 27]. This evidence displays the fact that although hypomethylation occurs on a global scale, hypermethylation may be seen when AD is studied in a gene-by-gene manner [26]. A final factor providing evidence for an epigenetic alteration contributing to AD pathology is the findings in a recent expression study showing over and under expressed mRNA levels from several genes that are associated with processes that are malfunctioning in AD [28]. These expression changes could be a result of epigenetic

changes in the promoter region of these genes. Together, these factors provide a strong argument for an epigenetic impact on the development of AD, but specific epigenetic effects have not yet been determined. If determined, these specific pathological alterations could not only give insight into the molecular pathology behind the development of AD, but they could also provide a signature to help in the early determination of AD, as well as in the target and development of future therapies. The hypothesis of this study is that various promoters in neurons affected by AD will display alterations in their methylation status, whether that be hypomethylation or hypermethylation, and that some of these promoter regions will be linked to genes that are associated to the pathology displayed in AD.

It should be noted that previous studies have sought to determine transcriptional changes in the genome of in vitro and in vivo AD models developed through beta amyloid treatment. However, these models were limited due to using undifferentiated neuroblastoma cells [29] or due to the fact that only small portions of the genome were analyzed in studies using mouse models [30]. The models described in this study dismiss these previous limitations due to their complexity and entirety. First, a differentiated neuroblastoma cell line was studied on a genomic and gene-by-gene basis. Due to the positive results obtained from this first study, a second study was performed using a transgenic mouse model that once again worked towards the complexity of a human in vivo model and once again studied DNA methylation on a genomic and gene-by-gene basis. Therefore, this study sought not only to look at a model that more accurately resembles the genome of a human affected with AD, but also to determine the specific molecular functions impacted by epigenetic promoter-based methylation changes.

Determining Methylated Genomic Regions

The basis of this study requires the ability to distinguish between the presence and absence of methylation in genomic regions. There have been several experimental methods used for determining the presence of DNA methylation, a few of which will be discussed here along with their positive and negative aspects. First, bisulfate sequencing is a method that uses sodium bisulfate to cause a reaction with unmethylated cytosine bases in a DNA strand resulting in sulfonated cytosine [31]. Once deaminated, the sulfate is removed from the produced sulfonated uracil. The DNA is then put through a polymerase chain reaction (PCR) that uses Taq polymerase, which identifies uracil as thymine. This causes the resulting PCR product to incorrectly display thymine at the genomic position of all unmethylated cytosines that have been converted to uracil [32]. However, methylated cytosine prevents the conversion of cytosine to uracil, resulting in PCR results that correctly label cytosine bases. This method is reliable, but impractical for genomic wide studies due to huge time and monetary requirements.

A similar method uses bisulfite sequencing and primers to determine where methylation exists [33]. Templates are treated in the manner described above except that instead of using Taq polymerase, methylation-specific primers are used to bind to cytosines that remain after the bisulfite treatment due to methylative protection. A PCR product reveals that a region is methylated due to the implication that the primer was able to bind. However, this method is still impractical for a genome wide study.

A third method takes advantage of the specific activity of methylation-sensitive restriction endonucleases (MSRE), which are enzymes that cut DNA specifically when certain methylation states exist [34]. Using two different MSREs that are isoschizomers

that both target 5'-CCGG-3' sequences, the methylation status of a specific region can be

determined. For example, HpaII recognizes and cuts 5'-CCGG-3' sequences only when

the cytosine is not methylated [34]. If the cytosine is methylated, it protects the DNA

from enzymatic cutting by HpaII. However, MspI cuts the DNA strand regardless of

whether it is methylated or not. Using a method called the HELP assay (**H**paII tiny

fragment **E**nrichment by **L**igation-mediated **P**CR), the fragments from the MSRE

digestions are co-hybridized to genomic microarrays [35, 36]. This allows for comparison

of the methylation status of intergenomic and intragenomic regions on a genome wide

scale making the HELP assay a practical and reliable method for genomic wide analysis

[37]. For this reason, this method was used in both the in vitro and in vivo models of the

presented study. However, there are limitations of this method that should be noted. First,

the HELP assay is limited to assessing the methylation status of CpG sequences that

reside in the restriction site 5'-CCGG-3'. Any methylation that exists on cytosine bases

outside of this sequence cannot be detected by this method. Also, this method requires a

fragment that is less than 2kb in size because fragments longer than that will not be

amplified by ligation-mediated PCR (LM-PCR) and therefore would not show up on the

microarray data. It is also likely that very small fragments (<20 base pairs) with high

internal complementarity will not ligate to LM-PCR primers due to their secondary

structure.

The final method for methylation determination that will be discussed is called

methylated DNA immunoprecipitation (MeDIP). This method uses an antibody to

specifically bind to methylated cytosines of fragmented DNA and allow for separation

from the rest of the DNA [38]. These separated fragments are then determined by

hybridization to a genomic chip array, which, like in the HELP assay method, makes this a practical approach to determining methylation statuses in a genome wide study. The MeDIP method does not have the limitation for there to be a 5'-CCGG-3' sequence due to the antibody only requiring cytosine methylation to allow it to bind. This method also eliminates the problem of inadequate fragmentation because it uses sonification, a technique that shreds the genome into many smaller fragments (200-1000 base pairs). Nonetheless, the HELP assay is more efficient at picking up small fragments due to the complex purification process of the MeDIP method, which could cause failure to detect CpG regions that are significant in the molecular processes causing development of AD. Regardless of its ability to have a broad and narrow focus as well as being reliable, due to expense, this method was only used in the in vivo transgenic mouse study.

One pitfall of both of the methods that were used (HELP assay and MeDIP) is that some CpG regions that demonstrate an altered methylation status may ultimately not regulate the transcriptional level of a nearby gene or the local chromatin structure. With that said, the altered methylation pattern could still serve as an indicator of AD development.

Alzheimer's Model Used for Each Study

IMR-32 cells were grown by ATCC prior to purchase using methods previously reported [39]. The IMR-32 cell line was chosen to serve as the in vitro cell model, which was completed prior to the start of the in vivo study. The IMR-32 cell line was chosen due to having the ability to be differentiated into cholinergic neuronal cells [40]. This type of neuron has receptors for acetylcholine and is able to secrete the Aβ protein, a function that is disrupted in AD leading to harmful effects caused by beta amyloid

aggregates. A portion of the differentiated IMR-32 cells was treated with Aβ protein to function as an AD model [26], while another portion of IMR-32 cells was left undifferentiated to act as a control for the differentiation procedure.

The in vivo model that was studied after completion of the in vitro model study consisted of two strains of mice obtained from the Jackson Laboratory. The first strain (B6SJL-Tg[APPSwFlLon,PSEN1*M146L*L286V]6799Vas/Mmjax) expresses two transgenes regulated by neural-specific elements to limit the overexpression to the brain. Expression of mutant Amyloid Precursor Protein (K670N, M671L, I716V, and V717I) and mutant Presenilin1 (M146L and L286V) results in the accelerated deposition of the 42 amino acid form of beta amyloid [41]. This provides pathology which mirrors that displayed in AD patients. These mice have memory impairment in the Y-maze test and recapitulate many of the major features associated with AD as reported by the Mutant Mouse Regional Resource Centers. The other strain used in this study does not express the transgenes but is of the same genetic background (B6SJL) to allow it to act as an accurate control. All mice used are age-matched and obtained from the Jackson Laboratory as adults (9-10 months old).

Materials and Methods

Brief Procedural Overview

The first step in the in vitro (IMR-32) study was the culturing and differentiation of the cell model. This step was unnecessary in the in vivo (transgenic mouse) study due to the mice being pre-prepared by the Jackson Laboratory. After this process, in both studies, the cells were harvested and the DNA was isolated and purified using the procedure described below. Once isolated, the DNA was digested with HpaII and MspI,

which are MSRE isoschizomers, to fragment the DNA based on the methylation status of 5'-CCGG-3' sequences. These fragments were then amplified using a method called the HELP assay, which as discussed previously, attaches adapters of known sequence onto the ends of fragments allowing for primer facilitated amplification. These amplified DNA samples from both studies were sent to professional laboratories, where they were fluorescently labeled and co-hybridized on promoter microarrays. Computer software was used to measure fluorescence and subsequently determine and graph HpaII/MspI ratios for each probe. This NimbleGen provided data was confirmed through PCR analysis of randomly chosen regions. The genomic regions with extreme methylation changes between control and disease state were linked to nearby genes, which were then linked to ontological function. A second method of analyzing DNA methylation in genomic promoter regions, MeDIP, which was discussed previously, was subsequently performed only in the transgenic mouse study. DNA was shredded into fragments using MseI and then treated with an antibody that binds to fragments by way of their methylated cytosines. The fragments that are bound by the antibody were then expressed as a purification enrichment by again using an outside laboratories microarray hybridization procedure. This data was analyzed by computer software based on fluorescence and revealed regional peaks of methylation change, which was once again confirmed through PCR analysis and assessed for significant gene ontology associations.

Isolation and Purification of IMR- 32 DNA

After the IMR-32 cells were grown by and purchased from ATCC, the cells were subsequently depleted of fibroblasts using immunomagnetic anti-fibroblast microbeads and LD MACS separation columns as was recommended by the manufacturer. Three

plates containing IMR-32 neuroblastoma cells were grown in proliferation medium

(DMEM with glutamax, 5% FCS, 100 U/ml penicillin-streptomycin, and 10 ug/ml

gentamicin) at 37C and 5% CO_2 for two days at a density of 5 x 10^6 cells/15 cm plate.

Two plates were then grown in differentiation media (DMEM with glutamax, 2% FCS,

2mM sodium butyrate, 100 U/ml penicillin-streptomycin, and 10 μg/ml gentamicin) for

seven days to allow for differentiation into mature neuronal cells. The last plate of

undifferentiated neuroblastoma cells was maintained in culture as a control for the

differentiation protocol. After the differentiation, one of the two plates was maintained,

and the other was treated with 25 μM AB_{1-40} peptide, as was previously reported [26], for

2 days to provide a model with one of the major pathological features of AD. The cells

were washed with cold PBS and isolated by scraping and centrifugation.

The nuclei pellets were stored at 80°C until the DNA extraction procedure was

carried out. At this point, approximately 100 μL of each type of nuclei pellet was thawed

and 478 μL of stop buffer [20% SDS; 5M NaCl; 0.5M EDTA], 20 μL protease K

[2.5mg/mL], and 2 μL RNase A [10mg/mL] were added. After gentle mixing, the

samples were incubated overnight in a 42°C hot water bath to allow for complete

degradation of cellular protein. 500 μL of PCIAA (Phenol-chloroform-isoamyl alcohol)

was added to each, followed by gentle mixing and incubation on a rotary wheel at 37°C

for 10 minutes. The samples were then centrifuged at 17,000xg for 5 minutes to cause

separation into aqueous and organic layers. The aqueous layer from each sample, about

400 μL, was transferred to a new eppendorf tube and saved. This PCIAA purification step

was repeated two more times for each sample.

The DNA was precipitated in each sample by adding NaOAc [3M] (equal to

1/10th sample volume), 100% ethanol (equal to 3x sample volume), and 1 µL of glycogen [20mg/mL]. The DNA in each sample was then pelleted by mixing and centrifuging at 17,000xg for 1 hour. The supernatant was removed through careful suctioning, and the DNA pellet was washed with 70% µL ethanol. The pellets were then resuspended in 200 µL deionized (DI) water. The DNA was stored at -20°C to protect from degradation. The concentration of the DNA in each sample was found using UV spectroscopy.

Isolation and Purification of Transgenic Mouse DNA

The in vivo model (transgenic mouse model) was ordered from Jackson Laboratory with all treatment and tests previously performed. The mice were kept for several days to determine that the mice were otherwise healthy in order to prevent any secondary health problems from skewing the data. After this time period, the mice were euthanized using CO_2 and decapitated. The brain was isolated immediately, sliced longitudinally, and placed in 60 mL of room-temperature 80% ethanol for 40 minutes, The hippocampi were then aseptically dissected on an ice-cold sterile platform. Both sides of the brain were kept on ice the entire time. The hippocampi were stored dry at -80°C. The DNA was then isolated from the control and disease state cells and purified using almost the same procedure as was described previously for the in vitro study except for two things. First, the pK stock used during the isolation of DNA was 20 mg/mL instead of 2.5 mg/mL as was used in the IMR-32 DNA isolation. Also, 1 µL of RNase and 10 µL of pK were added halfway through the isolation reaction to allow for more complete degradation.

HELP Assay

Portions of the DNA from all samples of both the IMR-32 and in transgenic

mouse study were digested with either HpaII or MspI MSREs. The HpaII digestion

reactions consisted of 1 µg of DNA, 4 µl of HpaII (10,000 U/ml), and 20 µl of New

England Biolabs Buffer 1, and the MspI digestions consisted of 1 µg of DNA and 2 µl of

MspI (20,000 U/ml) with 20 µl of NEB 4. Both reactions were raised to final volumes of

200 µl using DI water. The digestion was then allowed to incubate overnight in a hot

water bath at 37°C. The digested DNA was then purified using the methods described

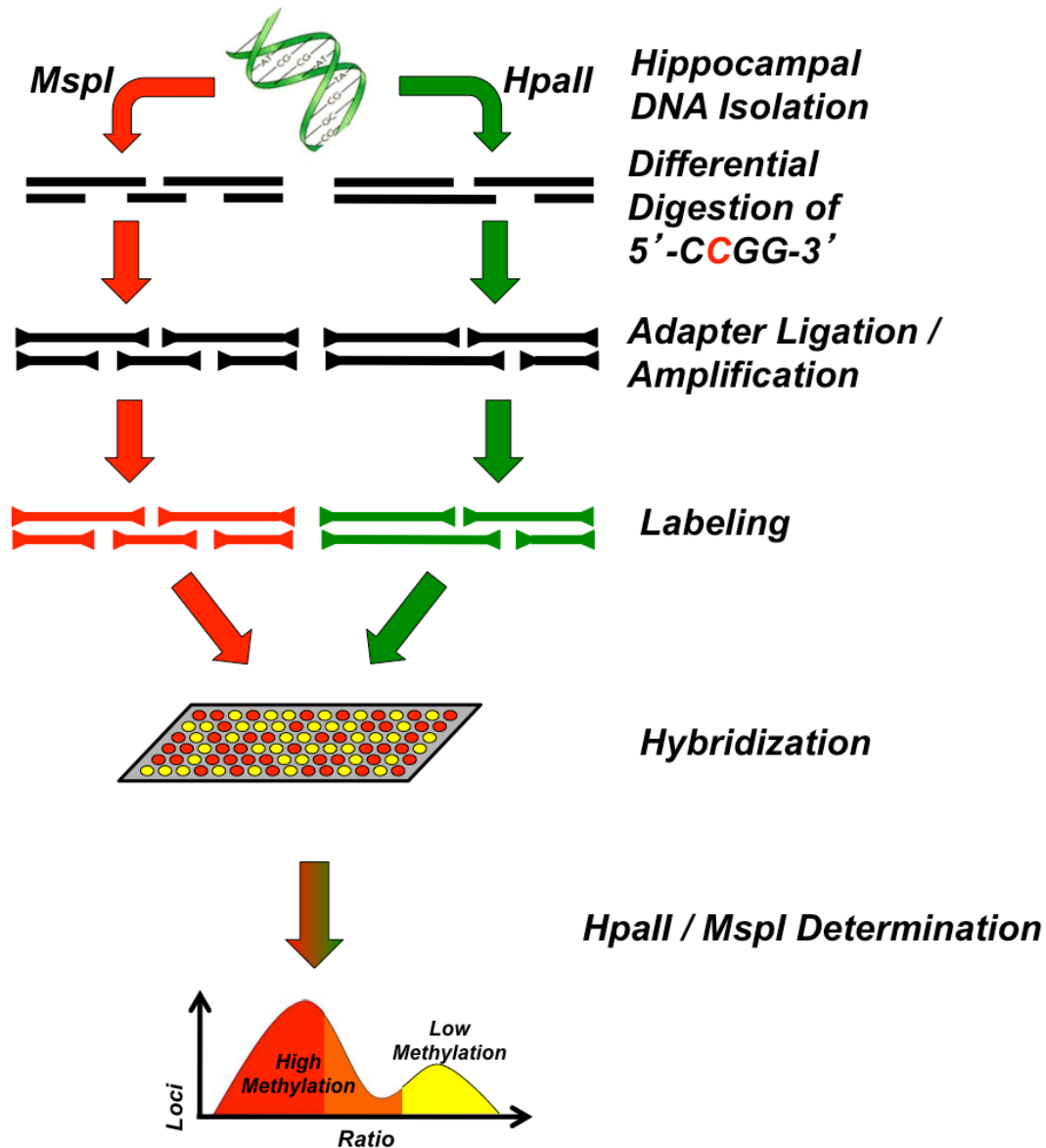previously and resuspended in 15.5 µl of 10 mM Tris-HCl (pH 8).

Ligation of adapters to allow for PCR amplification of the digested DNA was

carried out using two double stranded adapters, JHpaII and NHpaII. These adapters were

added to the DNA at concentrations of 40 mM each and were ligated to the ends of the

fragmented DNA using T4 DNA ligase. The sequence of JHpaII is 5'-

CGGCTGTTCATG-3' annealed to 5'-CGACGTCGACTATCCATGAACAGC-3', and

the sequence of NHpaII is 5'-CGGCTTCCCTCG-3' annealed to 5'-

GCAACTGTGCTATCCGAGGGAAGC-3'. The ligation reaction was carried out in

PCR tubes and consisted of 6 µl of 5× T4 ligase buffer (250 mM Tris-HCl (pH 7.6), 50

mM MgCl$_2$, 5 mM ATP, 5 mM DTT, 25% (w/v) polyethylene glycol-8000, Invitrogen),

15.5 µl digested DNA, 4 µl of 50 µM pre-annealed JHpaII linkers, 4 µl of µM pre-

annealed NHpaII linkers, and 1 µl of T4 DNA ligase (4 U/ µl). The reactions were put in

a thermocycler at 16°C overnight. The reactions were then diluted to 10 ml by 10 mM

Tris-HCl (pH 8).

For the ligation mediated PCR, twice as much digested DNA was used for HpaII

samples than was used for MspI samples due to differences in the digestion products. The

MspI digestion causes more complex fragments that result in quicker amplification and

therefore premature saturation. This would mean unwanted elements developed during

"excess" PCR cycles could contaminate the solution. However, the decreased DNA

content in the MspI samples eliminated this problem. The LM-PCR reaction contained 5

µl of HpaII digested DNA or 2.5 µl of MspI digested DNA, .5 µl of JHpa 24-mer

oligonucleotide, .5 µl of NHpa 24-mer oligonucleotide, 25 µl of Supermix (Bio-Rad), and

brought to a final volume of 50 µl with DI water. The two longer primers will be used to

amplify 1/50 of the ligated fragments by qPCR using EvaGreen Supermix (Biorad). The

following cycle arrangement was used: 10 minutes at 72°C, 20 cycles of 30 seconds at

95°C and 3 minutes at 72°C, and a final 10 minutes at 72°C.

        After another purification process using a Qiagen QIAquick PCR purification kit,

the DNA samples from both studies were measured out into portions equaling final

masses of at least 4 µg of DNA and concentrations of at least 250 ng/µl. The DNA

fragments from each DNA sample (2 IMR-32 undifferentiated, 2 IMR-32 differentiated,

1 IMR-32 Aβ treated) were fluorescently labeled and hybridized to promoter arrays

manufactured by NimbleGen (2.1M Deluxe Promoter Array). These arrays contained

DNA sequences representing 10kb of all annotated promoters (spanning from 7kb

upstream and 3kb downstream of the transcription start site) and included 28,266 CpG

clusters and 475 miRNA transcripts.

Figure 1. HELP Assay Overview. DNA was isolated from IMR-32 undifferentiated, differentiated, and beta amyloid treated cells as well as from hippocampal cells from transgenic mice overexpressing beta amyloid and their control counterparts. The DNA was either digested with HpaII or MspI and then ligated to adapters of known sequence using Taq polymerase. The DNA was amplified using LM-PCR and then sent to NimbleGen (IMR-32) or Arraystar (Transgenic Mice) where it was fluorescently labeled and hybridized to a promoter microarray. Probe fluorescence was measured and HpaII/MspI probe value ratios were analyzed and graphed using Matlab 2011.

HELP Assay Microarray Analysis for IMR-32 Study

Matlab 2011 was used for the analysis of the raw microarray data. Briefly, the pairwise data files supplied by ArrayStar were used to calculate the log ratio data (HpaII / MspI) for each array. Mean centered histograms were generated from the log ratio data. Since MspI fragments represent the universe of possible fragments, array regions that failed to give a signal in the MspI sample were excluded from the analysis. The ratio values were then subjected to lowest normalization and the arrays were normalized to each other using equivalent sum of squares scaling. An error model was generated using a 600 base pair moving window with 150 base pair steps in which both the mean probe log ratio and p-value were calculated for each window. [42] This method summarized the local intensity of amplified fragments when multiple oligonucleotides were representing the fragment. All p-values were calculated using a nonparametric Wilcoxon signed-rank test. In order to establish an initial significant ratio threshold (for hypermethylated and hypomethylated designations), an HpaII / MspI log ratio density plot was generated and averaged across all array replicates. Subsequently, due to there being only 1 sample of Aβ treated, this data was not averaged with any other data set. This type of plot produced a bimodal distribution of ratio occurrences and allowed a log ratio threshold to divide the two modes [37]. Genomic regions that contained ratios greater than this threshold and have a p-value <0.05 were designated as hypomethylated regions. Genomic regions that contained ratios less than this threshold and have a p-value <0.05 were designated as hypermethylated regions. The most changing 0.1% of all the regions, the 0.05% of regions undergoing the most loss of methylation, and the 0.05% of regions undergoing

the most gain of methylation, were chosen as the regions of interest for this study due to this list's extreme stringency (refer to Figure 3).

HELP Assay Microarray Analysis for Transgenic Mouse Study

After amplification by LM-PCR as was described previously, the DNA from the control and disease-state transgenic mice was again purified, as in the IMR-32 study, and measured out to final masses of at least 4 µg of DNA and concentrations of at least 250 ng/µl, as specified by the microarray manufacturer. The DNA fragments from each DNA sample (2 control transgenic mice and 2 disease-state transgenic mice) were fluorescently labeled and hybridized to promoter arrays. This study used a different type of NimbleGen promoter array, Multiplex MM9 CpG Promoter Array, which is designed for mouse genomes. These arrays contained DNA sequences representing 20,404 annotated promoters (spanning from 3kb upstream to 0.7kb downstream of the transcription start site) and included 15,980 CpG islands. This data was assessed using Matlab 2011, as previously described for the IMR-32 study.

Gene Ontology Assessment for HELP Assay in Both Studies

Gene symbols were linked to the 0.1% most changing microarray probes, 0.05% probes becoming hypomethylated and 0.05% probes becoming hypermethylated, by plugging the region of that probe into GREAT, a region/gene association and annotation software developed by Stanford University and Bejerano Lab. Human genome 18 was used for the species assembly in the IMR-32 study, and mus musculus 9 was used for the species assembly in the transgenic study. The whole genome was used for the background regions. This software developed graphs representing the number of associated genes per region, distance to TSS, and absolute distance to TSS. Under the

global controls options, "View all region-gene associations" was chosen to obtain all of

the gene symbols for the inputted regions. These gene symbols were then plugged into

GeneCodis, a gene annotation website; homosapiens was used as the organism and

biological processes was selected for genome wide assessment. The gene symbols linked

to the 0.05% probes becoming most hypomethylated, the 0.05% probes becoming most

hypermethylated, and a random list of genes of equal size to the lists being evaluated

were assessed using the following G.O. requirements: level 7 (the most stringent), a

minimum of 3 genes associated with that ontology, and a chi square value that was lower

than the lowest obtained chi square value from the random list that was associated with

specific ontology topics. These topics included neurological related functions and

apoptosis. False discovery rate was used to find a corrected chi square value. The

enrichment value was calculated by dividing the ratio of genes for a gene ontology

category in the list to the total number of genes in the list by the ratio of genes for that

gene ontology category in the genome to the total number of genes in genome as

demonstrated by the following formula:

$$\frac{\left(\dfrac{\text{Number of Genes for G.O. in List}}{\text{Number of Genes in List}}\right)}{\left(\dfrac{\text{Total Number of Genes for G.O.}}{\text{Total Number of Genes in Genome}}\right)}$$

The gene ontologies that met these requirements were charted along with their linked

gene symbols and calculated chi-square and enrichment value. [42]

**MeDIP Assay for Transgenic Mouse Study**

A portion of the DNA isolated from the transgenic mice was also assessed using

methylated DNA immunoprecipitation. Instead of digestion with HpaII and MspI, the

DNA from the 2 control and 2 AD mice was sent to Arraystar in total amount and

concentration equal to that of the HELP assay microarray procedure. It was then shredded into fragments of about 200-1000 base pairs using sonification. Immunoprecipitation of methylated DNA fragments was carried out using Biomag magnetic beads coupled mouse monoclonal antibody that binds to methylated cytosine. Control sequences were mixed in with the genomic fragments. The immunoprecipitated DNA was isolated from the unbound DNA and purified as previously described using phenol chloroform extraction and ethanol precipitation.

The methylated DNA fragments were then fluorescently labeled with Cy3- and Cy5- labeled random 9-mers. These fragments were hybridized to NimbleGen Mouse 3x720K Promoter Plus CpG Island Arrays, which is a single array design that includes 15,980 CpG Islands and 20,404 RefSeq gene promoter regions (from about -2960bp to +740bp of the TSSs). This array contained a total of approximately 720,000 probes. An Axon GenePix 4000B microarray scanner was used to scan and compute the fluorescence given off by each probe.

MeDIP Microarray Analysis for Transgenic Mouse Study

Differentially methylated regions were determined by performing a T-test on different groups of replicate samples to calculate the p-value for each probe. Those p-values <0.05 were defined as differentially methylated probes, which were then further analyzed to find differentially methylated regions (DMR). Simply stated, the DMRs are those regions that show significant changes in the methylation status of a sequence of probes' values between the control and AD genome. All of the DMRs between both assays were combined into one list that provided the region of the genome where the peak of changing probes exist, the gene symbol that this region is linked to, NM and NP
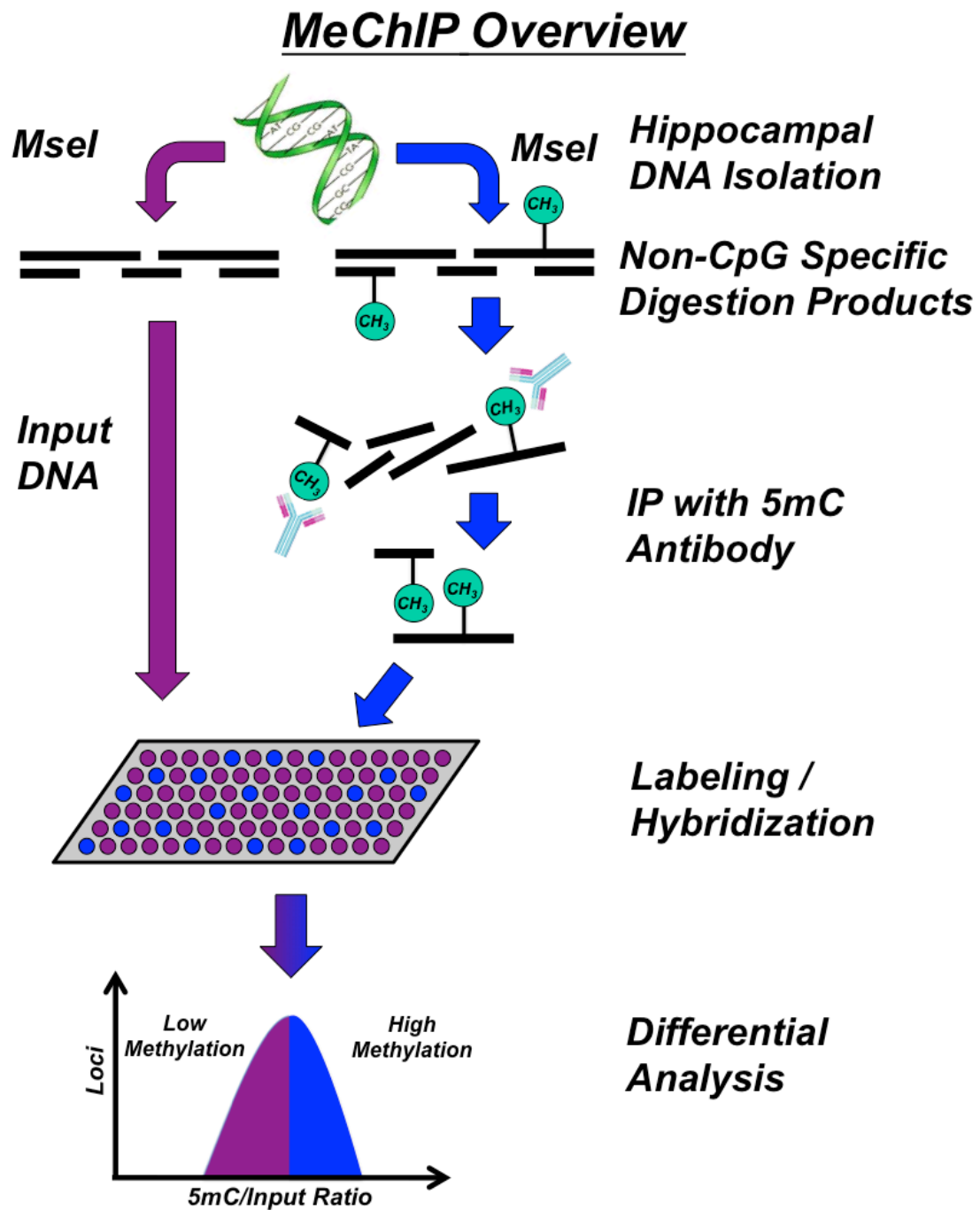
Figure 2. MeDIP Assay Overview. DNA was isolated from hippocampal cells from transgenic mice overexpressing beta amyloid and their control counterparts. This assay was not carried out in the IMR-32 study. The DNA was then sonicated into fragments of 200-1000 base pairs. Methylated fragments were isolated using a monoclonal antibody that binds to methylated cytosines. These fragments were sent to ArrayStar where they were fluorescently labeled and hybridized to a promoter microarray. Fluorescence was measured and regions with significant changes in methylation levels were reported.

numbers, the assay that the data came from, and the distance of the DMR from the

transcription starts site (TSS) and transcription termination site (TTS). Once this data was

provided by Arraystar, the list of DMRs was narrowed down using Microsoft Excel 2010

to only those genes that were linked to DMRs in their promoter regions that were mapped

to within 500 base pairs of each other in both assays.

Gene Ontology Assessment for Transgenic Mouse Study

Genecodis, a gene annotation website, was again used. However, the use of

GREAT was not necessary for this assay due to the DMRs being previously linked to

their associated genes. Mus musculus was used as the organism and biological processes

was selected for genome wide assessment. The gene symbols of the regions becoming

more hypomethylated, more hypermethylated, and a random list of equal size to the lists

being evaluated were assessed using the same G.O. requirements as in the HELP assay.

The random list was pulled from a list of all gene-linked promoter transcripts provided by

Arraystar. False discovery rate was again used to find a corrected chi square value, and

the enrichment value was calculated using the same formula presented previously. The

gene ontologies that met these requirements were charted along with their linked gene

symbols and calculated chi-square and enrichment value.

Confirmations of Microarray Data in Both Studies

MSRE digestion and qPCR analysis of digested DNA were used to confirm the

HELP and MeDIP microarray data from both studies. Some regions that were confirmed

in the IMR-32 study were randomly chosen, while others were chosen based on having

significant biological functions as discovered in the gene ontology assessment. The

randomly chosen regions were pulled from a list of the most changing 0.1% of all the

regions, the 0.05% of regions undergoing the most loss of methylation, and the 0.05% of

regions undergoing the most gain of methylation. All of the confirmations carried out in

the transgenic study were specifically chosen based on significant biological function. All

of the confirmations focused primarily on the change between the HpaII/MspI ratio

between control and AD DNA.

   To carry out these qPCR site-specific confirmations, primers were designed using

the UCSC genome browser, ApE, and Primer3. The UCSC genome browser was used to

determine the specific DNA sequence around the probe or of the region being confirmed.

ApE (A Plasmid Editor) was used to highlight the 5'-CCGG-3' sequences in the region

being confirmed. The primers were then designed using Primer3 (http://biotools.umass

med.edu/bioapps/primer3_www.cgi). They were specifically designed around the 5'-

CCGG-3' sequence nearest the probe or probes showing extreme change in their

methylation status. The primers were designed around this sequence specifically because

it is targeted and shredded by the enzymes being used based on the methylation status.

The specific requirements set while designing the primers were as follows: product size

range was chosen to be between 80-140 base pairs, the primer T_m was 60 ± 2, and the

primer size was 20 ± 2 base pairs. All other criteria were left as the default settings by the

software. The following stipulations were required for a region to be confirmation

qualified: a CCGG close to a changing probe and the possibility for primer design within

the previously stated primer design requirements.

   The control and Aβ DNA from both studies were digested with HpaII, MspI, and

50% glycerol (to act as a control) in separate reactions. The HpaII digestion reactions

consisted of 2 µg of DNA, 8 µL of HpaII, 40 µL of NEB Buffer 1, and raised to 200 µL

using DI water. The MspI digestion reactions consisted of 2 μg of DNA, 4 μL of HpaII, 40 μL of NEB Buffer 1, and raised to 200 μL using DI water. The glycerol control reaction mirrored the MspI reaction except that it contained 2 μL of 50% glycerol instead of MspI. These digestion reactions were incubated overnight in a hot water bath at 37°C and then purified using the PCIAA procedure described previously. The samples were stored at -20°C after being raised to 200 μL in DI water.

The qPCR confirmation reactions performed in a BioRad MJ Mini Personal Thermal Cycler contained the following: .015-.025 μg of either HpaII or MspI digested DNA or uncut DNA from the glycerol digestion, primer working stock that contained .625 μM of both the forward and reverse primer, 12.5 μL of BioRad Supermix. This reaction was raised to 25 μL in DI water. [42] Control reactions, which lacked DNA, were also run to confirm that primer self-annealing and amplification were not occurring. The touchdown PCR cycle started with a 5 minute melting step at 95°C. This was preceded by a cycle consisting of a 10 second melting step at 94°C, followed by a 30 second annealing period at 69°C, and a 30 second extension step at 72°C. This cycle was repeated 19 times, but each time the annealing step decreased by .5°C. This was followed by a second cycle consisting of a 10 second melting step at 94°C, a 30 second annealing at 59°C, and a 30 second extension step at 72°C. This second cycle was repeated 24 times, but the annealing step temperature was held constant. The touchdown qPCR reaction was concluded with a 5 minute extension step at 72°C. BioRad CFX Manager 2.0 was used to develop amplification graphs. [42] To determine the cycle in which each of the DNA amplifications of a specific confirmation reached equivalent concentrations, a horizontal line was placed through the point at which each sample's (uncut, MspI, and

HpaII) amplification was in its most linear phase. This was carried out for each of the

confirmations, and the cycle quantification was recorded for use in graphing the

difference between the HpaII and MspI amplification speeds.

Results

Aβ Induction Results in Little Genomic Scale Methylation Alteration

Analysis of genome-wide promoter methylation levels provided by the microarray

allowed for production of distribution graphs for the control and disease states of both

models, representing hypomethylated and hypermethylated promoter CpG dinucleotides.

These graphs plotted the control and Aβ microarray probe $\log_2$ HpaII/MspI ratios as

frequency distributions and mean-centered all of the ratios at zero. Positive ratios

represent loci that are less methylated than the mean, and negative ratios represent loci

that are more methylated. The curves represent the probability of the data from each bin

belonging to the corresponding peak. [42] The mean HpaII/MspI ratios of the control and

diseased state peaks were calculated and are as follows: -0.66 and 1.76 for the control

IMR-32 microarray, -0.76 and 1.95 for the Aβ treated IMR-32 microarray, -0.195 for the

control transgenic mouse microarray, and -0.267 for the Aβ overexpressed transgenic

mouse microarray. It should be noted that the IMR-32 study contained two peaks in each

of the distribution graphs due to it being a cancer cell line. The epigenetic makeup is

previously altered from the norm due to the cancer disease state. Therefore, the

transgenic mouse model distribution graph, which contains only one peak, is a much

more accurate representation of the epigenetic makeup before and after AD development.

The distribution between the control and disease state in each model were extremely

similar, with an r^2 value of 0.978 for the IMR-32 study and 0.8763 for the transgenic

mouse study. Together, this data provides evidence that Aβ treatment does not have a large global impact on DNA methylation levels, but instead impacts a small number of gene promoter methylation statuses.

Methylation Changes at Discrete Genomic Loci

Due to the promoter methylation levels not showing a large impact on a genomic scale, these studies focus on the impact of epigenetic changes at specific genomic loci. To assess only the extreme changes at specific loci, a histogram was generated that plotted the difference resulting from the subtraction of the control microarray data from the Aβ treated microarray data in a $\log_2$ form. Ratios greater than zero illustrate probes becoming hypomethylated, and those less than zero illustrate probes becoming hypermethylated. This data works to further support the conclusion that little change is occurring on a genomic scale due to most of the data being around zero, therefore undergoing little change. It also displays those regions undergoing drastic change, highlighting the primary focus of these studies.

Confirmations of randomly chosen regions in the IMR-32 study were performed after mapping the microarray region and designing primers around 5'-CCGG-3' sequences in close proximity to probes undergoing extreme change. For example, primers were designed around a probe in the genomic region chr13:113568450-113569450, a region becoming hypermethylated according to the microarray data. qPCR resulted in amplification of HpaII digested control DNA that almost matched that of the MspI digested control DNA. This showed that this region contained little methylation in the control state due to HpaII being able to cut to almost the same extent as MspI, which can cut all the time regardless of methylation status. However, when the same qPCR reaction

was run with Aβ treated DNA, the HpaII digested DNA showed very slow amplification

in comparison to the MspI digested DNA. This slow amplification was due to

methylation blocking HpaII's cutting ability, resulting in fewer fragments for

amplification. This data suggests that the region is gaining methylation as a result of Aβ

treatment. The opposite results were determined when site-specific qPCR was performed

on chr17:54996867-54998139, a genomic region that was becoming hypomethylated

according to the microarray (refer to Figure 3). Random confirmations using qPCR,

MSRE digested DNA and designed primers provided results showing that 44 of the 45

confirmations supported the microarray data, giving further confidence in the microarray

results (refer to Figure 5). Confirmations were then performed on 5'-CCGG-3' located in

promoter regions of genes linked to significant ontology categories provided by

Genecodis, which also supported the microarray data. The significance of these

epigenetic changes occurring in genes linked to significant ontological categories will be

examined in the discussion.

Promoter Methylation Changes Occur in Regions Proximal and Distal to the TSS

As mentioned previously, GREAT, a region/gene association and annotation

software developed by Stanford University and Bejerano Lab, mapped the distance of the

regions of interest (most changing 0.1%) from the TSS (refer to Figure 4). This analysis

gave a wide variety of results, as some regions were mapped further than 10k base pairs

away from the TSS (e.g. DLX1), while others were mapped very close to the TSS (e.g.

VHL). As expected, due to using microarrays that focused primarily on promoter

proximal regions, many of the regions of interest showed changes occurring at promoter

proximal positions. For example, 45% of the regions undergoing a loss of methylation

were located within 5k base pairs of the TSS, whereas only 16% of the regions gaining

methylation were within this frame. [42] Future studies are needed to determine if certain

loci are more inclined towards a certain type of disease-linked epigenetic shift.
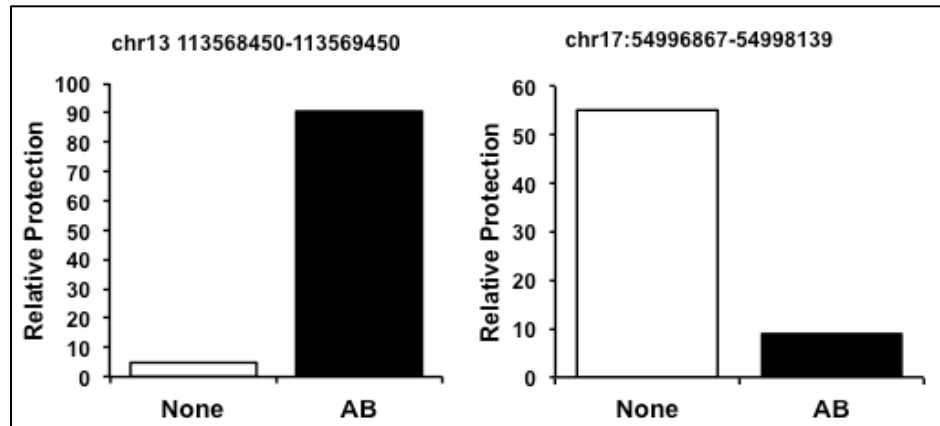
Figure 3. Confirmations of Randomly Chosen Region Showing Dramatic Change Support Microarray Data. qPCR was performed on MSRE digested control and Aβ treated DNA. A horizontal line was placed through the point at which each sample's (uncut, MspI, and HpaII) amplification was in its most linear phase to allow for determination of amplification speed. The cycle numbers for DNA samples of the same type (control and Aβ treated) provided by the horizontal line were graphed, and this HpaII/MspI ratio was then graphed against the HpaII/MspI ratio of the opposite DNA sample. These graphs, as shown above, allowed for comparison of methylation (protection) levels between control and disease state, therefore displaying the change brought about by AD development.
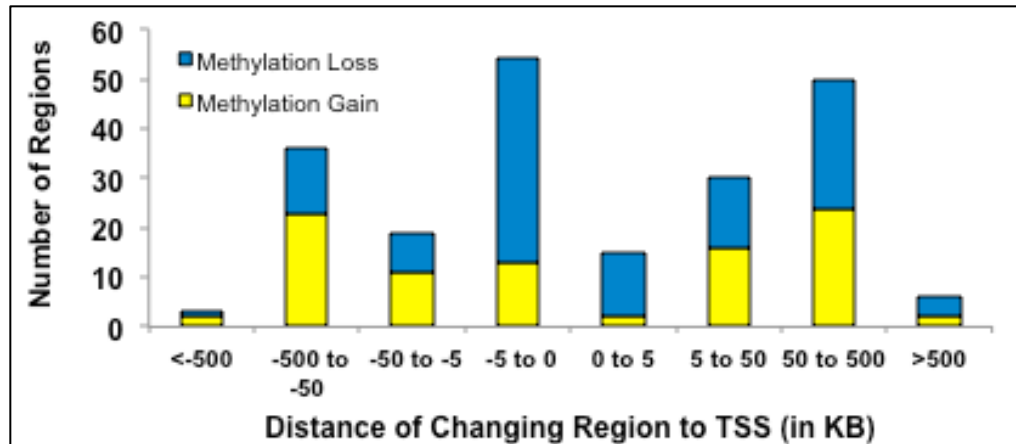
Figure 4. Promoter Methylation Changes Occur at Positions Proximal and Distal to the TSS of a Gene. This graph displays the number of regions experiencing a specific type of change, either methylation increase or decrease, at specific distances from the TSS as provided by GREAT. The x-axis represents the distance from the TSS in which those regions fall, while the y-axis represents the number of regions in a certain distance grouping. The color distinguishes whether a gain or loss of methylation is occurring at that region. Blue represents methylation loss, and yellow represents methylation gain.
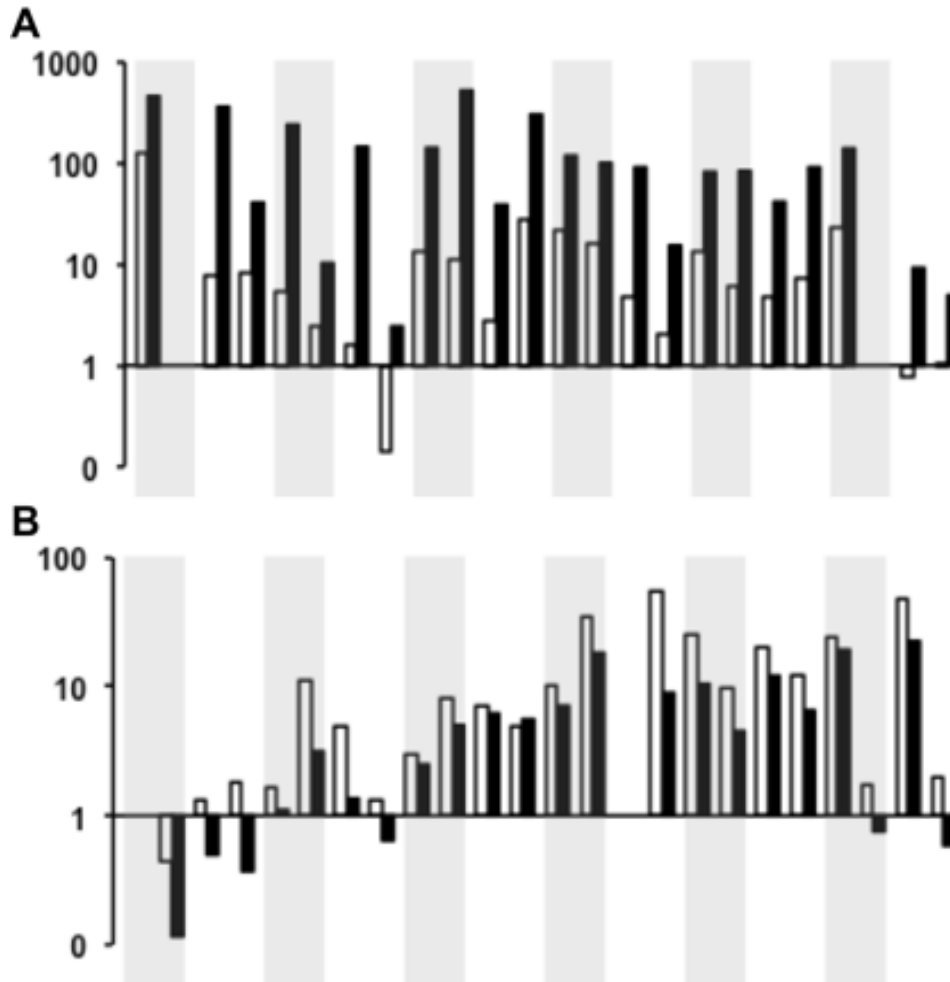
Figure 5. qPCR Confirmations of Regions Undergoing Change Support IMR-32 Microarray Data. The graphs above represent the 45 confirmations that were performed on regions randomly selected from a list of regions undergoing the most change between control and Aβ treated microarray data. The y-axis represents the amount of relative protection (due to methylation) that a region contains. The columns immediately next to one another represent the data being compared. The white columns represent the relative protection that exists in the control state, and the black columns represent the relative protection in the Aβ treated state. The graph on the top (A) represents the regions becoming hypermethylated (gaining protection) due to Aβ treatment, while the graph on the bottom (B) represents the regions becoming hypomethylated (losing protection) due to Aβ treatment. 44 out of the 45 (97%) regions tested confirmed the microarray data.

Promoter Alterations Are Linked to Genes with Significant Ontological Functions

Analysis of the ontological assignments linked to genes experiencing changes in their promoter methylation levels in both the IMR-32 model and the transgenic mouse model provided insight into functions being impacted by these alterations. Genecodis was used to assess the genes experiencing change in the HELP assays from both studies, as well as those in the MeDIP assay from the transgenic study. All of the lists showed genes involved in neuronal and cell fate functions, and the p-values of these results were compared to a random list to ensure mathematical significance (refer to Figures 6-8).

HELP Assay Ontology for IMR-32 Study

Genes Becoming Hypomethylated

Gene Ontology	Genes Involved	p-value	Enrichment
Neurogenesis CNS Neuron Differentiation Neuron Fate Commitment	Dlx1, Dlx2, Nkx6-2	<.001	192
Cerebral Cortex GABAergic Interneuron Fate Commitment	Dlx1, Dlx2	<.001	320
Reg. Nervous System Development	Mbp, Accn1, Nkx6-2	1.02×10^{-21}	38
Regulation of Neurogenesis CNS Development	Dlx2, Dlx1, Mbp, Nkx6-2	3.06×10^{-21}	28
Neg. Reg. of Apoptotic Process	Sox9, Vhl, Hand2	1.91×10^{-17}	30

Genes Becoming Hypermethylated

Gene Ontology	Genes Involved	p-value	Enrichment
Forebrain Development	Pcnt, Mapk8ip3, Ski	1.66×10^{-16}	29
Reg. of Apoptotic Process	Gas6, Lyst, Adam8	2.03×10^{-10}	18
Neurogenesis	Dll1, Pcnt, Mapk8ip3, Ski	7.89×10^{-10}	13

Figure 6. Beta Amyloid Treated Cells Show Methylation Changes in Genes Linked to Apoptotic and Neuronal Functions. GREAT, a region/gene association software was used to determine the gene symbols that were linked to the 0.1% most changing promoter regions. Genecodis, a gene annotation website, was then used to determine the ontological functions associated with these gene symbols. The table contains ontological functions that were associated with the gene list and have p-values for functions of the same topic that were lower than in a random list. The "Genes Involved" column displays the genes linked to the ontology category in that row. The p-value and enrichment demonstrate the likelihood that these genes linked to the same ontological category would exist in the same list of this size.

HELP Assay Ontology for Transgenic Study

Genes Becoming Hypomethylated

Gene Ontology	Genes Involved	p-value	Enrichment
Negative Regulation of Synapse	Wnt5a	4.47×10^{-28}	194
Neg. Reg. of Nervous System Development	Wnt5a	4.20×10^{-21}	129
Noradrenergic Neuron Differentiation	Phox2b	3.51×10^{-14}	78
CNS Neuron Development	Ephb3, Phox2b, Drd1a	4.57×10^{-14}	24
Dopaminergic Neuron Differentiation	Wnt5a	2.0×10^{-7}	35
Regulation of Axon Extension Involved in Axon Guidance	Wnt5a	6.50×10^{-7}	32
Brain/Neuron Development	Atf1, Dtnbp, Ephb3, Phox2b, Notch1, Nr2f6, Drd1a	7.71×10^{-7}	5

Genes Becoming Hypermethylated

Gene Ontology	Genes Involved	p-value	Enrichment
Positive Regulation of Cell Size	Rb1cc1	6.50×10^{-12}	65
Positive Reg. of Axon Extension	Trpv2	2.14×10^{-4}	21
Positive Regulation of Cell Growth	Trpv2, Cxcl16	2.23×10^{-4}	11
Positive Regulation of Neurogenesis	Gh, Trpv2	7.92×10^{-3}	7

Figure 7. Methylation Changes in Transgenic Mouse Model Demonstrated by the HELP Assay Results are Linked to Apoptotic and Neuronal Functions. This table demonstrates the ontological functions associated with genes linked to the regions showing the 0.1% most significant change from the HELP assay data in the transgenic mouse model. The genes linked to the listed ontological function are represented in the "Genes Involved" column. Refer to Figure 6 for details about p-value meaning and requirements, as well as enrichment calculations.

MeDIP Assay Ontology for Transgenic Study

Genes Becoming Hypomethylated

Gene Ontology	Genes Involved	p-value	Enrichment
Neurogenesis CNS Development CNS Neuron Differentiation	32 Genes*	8.40×10^{-16}	4.125
Axon Regeneration	Omg, Rtn4rl1, Jun, Rtn4	1.70×10^{-13}	20.289
Neuron Remodeling	Farp2, Ntn4	6.37×10^{-9}	25.924
Pos. Reg. of Mitochondrial Fission	March5	1.31×10^{-8}	59.877
Regulation of Apoptosis	27 Genes**	7.57×10^{-8}	2.911
Blood Vessel Endothelial Cell Proliferation Involved in Angiogenesis	Nrarp	1.28×10^{-6}	39.918
Gliogenesis	Nf2, Gli3, Omg, Sox6, Rtn4, Notch1, Klf15	5.97×10^{-6}	5.481

Genes Becoming Hypermethylated

Gene Ontology	Genes Involved	p-value	Enrichment
Natural Killer Cell Activation	Klrk1, Elf4, Itgb2, Hps1	8.96×10^{-14}	19.575
Pos. Regulation of Autophagy	Pim2, Ulk1	5.88×10^{-12}	34.255
Regulation of Neuron Apoptosis	Cited1, Agap2, Trp73, Agrn, Sncb, Kcnip3	1.21×10^{-5}	5.906
Neurotransmitter Receptor Metabolic Process	Agrn	1.72×10^{-5}	28.546
Regulation of Nervous System Development	Mt3, Serpinf1, Foxa1, Trp73, Chrd, Inpp5j, Agrn, Ulk1, Chn1	4.33×10^{-4}	3.495

*Mir 17, Fgf20, Mir19a, Nf2, Mir92-1, Gli3, Vax1, Dpysl5, Omg, Tomt, Sipa1l1, Ctdsp1, Farp2, Rtn4rl1, Otp, Mir18, Rbpj, Irx5, Isl2, Jun, Caprin1, Sox6, Lmx1b, Efna5, Mir19b-1, Rtn4, Notch1, Ntn4, Klf15, Emx2, Hook3, Mir20a
** Mir17, Mir92-1, Gli3, Tbx1, Itsn1, Plcg2, Mir18, Dcun1d3, Jun, Map3k5, Rbm5, Apip, Eaf2, Gpam, Mir19b-1, Jag2, Rtn4, Notch1, Asns, Ripk1, Furin, Msh6, Ercc1, Fadd, Dyrk2, Mir20a, Aars

Figure 8. Methylation Changes in Transgenic Mouse Model Demonstrated by the MeDIP Assay Results Are Linked to Apoptotic and Neuronal Functions. The genes showing extreme change in their promoter methylation levels in the MeDIP assay in both experimental samples were assessed for ontological function using Genecodis. This list consisted of 223 genes with promoter regions becoming hypermethylated and 330 regions becoming hypomethylated in their promoter regions. The genes linked to the listed ontological function are represented in the "Genes Involved" column. An excel-generated random list of equal size to the ones being analyzed was used to set a standard for what p-values were to be considered significant. Refer to Figure 6 for details about p-value meaning and requirements, as well as enrichment calculations.

Discussion

Several conclusions can be drawn from the results obtained from these studies of epigenetic alterations in promoter regions due to Aβ treatment or overexpression. First, global scale methylation levels are for the most part consistent between control and disease state models. The second conclusion pulled from these studies is that specific genomic loci do experience extreme promoter methylation changes due to Aβ treatment. The specificity of the alterations drew the focus of these studies to examining the impact of these changes. This leads to the last two conclusions, the latter of which will be the highlight of these studies. But the first calls for a brief mention, and that is the conclusion that epigenetic alterations happen all throughout the promoter region, regardless of distance to the TSS. As mentioned in the results, some regions undergoing change are located only a few hundred base pairs from the TSS, whereas others are around 15k base pairs away. However, the distal changes are also important due to evidence which shows that enhancer mechanisms can allow for distal regulation of gene transcription [43, 44]. Nonetheless, it should be mentioned that GREAT maps genes to the closest "canonical" TSS, so it may be closer to a different TSS that is not yet firmly established [42]. It should be noted that this data calls for more detailed research into genomic wide epigenetic alterations, rather than a promoter specific focus as this study carries out.

The last and most interesting conclusion is the ontological functions associated with the genes undergoing the most drastic promoter methylation alterations. As shown by Figures 6-8, all of the assays in both studies link the most significant changes to genes associated with neuronal and apoptotic processes. Due to these associations, it appears that epigenetic factors may be impacting AD pathology in a direct manner through

alterations in the normal transcription of several vital genes. To help highlight the importance of this finding, we developed models for how these epigenetic alterations may possibly change transcription and contribute to AD pathology.

For the IMR-32 study our model associates the alterations in the promoter regions of the DLX1, VHL, and PCNT genes to possible AD pathology. DLX transcription factors have been found to have a direct impact on the migration and differentiation of GABAergic interneurons [45]. In studies using DLX1/2 knockout mice, migrational disruption and premature neurite (axon and dendrite) growth were observed showing that activity of these neurons is necessary for proper migration and repression of neurite outgrowth in premature neurons. Ultimately, DLX1/2 help premature neurons keep a compact shape while migrating to allow for proper movement and placement. As for VHL, this gene is a tumor suppressor gene that down-regulates proliferation factors [46]. The last gene used to develop a model for the IMR-32 study is PCNT, which has been linked to promoting proper mitotic spindle assembly and metaphase progression in the cell cycle [47, 48]. In the IMR-32 study, DLX1 and VHL are becoming hypomethylated due to Aβ treatment, and PCNT is becoming hypermethylated. Therefore, our model suggests that transcriptional changes due to these epigenetic alterations would lead to de-differentiation or regression of neurite outgrowth, due to overexpression of DLX1, and lack of production or division of neural precursor cells, due to overexpression of VHL and under expression of PCNT. However, the IMR-32 study did not assess the mRNA levels of these cells, therefore the epigenetic based transcriptional alterations are only proposed. Nonetheless, this model does demonstrate the need for further investigation. As for the transgenic study, similar results have been found showing that many genes linked

directly to neuronal and apoptotic functions undergo epigenetic methylation alterations due to Aβ overexposure.

In conclusion, these studies provide evidence that warrants further study into the epigenetic basis of AD pathology, as well as research delving into the causes of these alterations. The determination that epigenetics plays a direct role in the pathology associated with AD development, would provide a target for future therapeutic methods. If these therapies could reverse the epigenetic shifts, it would be speculated that the pathology resulting from these shifts could also be reversed. However, the cause must be determined before a therapy can be discovered.

References

1.   Glenner, G.G. and C.W. Wong, *Alzheimer's disease: initial report of the purification and characterization of a novel cerebrovascular amyloid protein. 1984.* Biochem Biophys Res Commun, 2012. 425(3): p. 534-9.

2.   Singh, T.J., I. Grundke-Iqbal, and K. Iqbal, *Phosphorylation of tau protein by casein kinase-1 converts it to an abnormal Alzheimer-like state.* J Neurochem, 1995. 64(3): p. 1420-3.

3.   Alonso, A.D., et al., *Abnormal phosphorylation of tau and the mechanism of Alzheimer neurofibrillary degeneration: sequestration of microtubule-associated proteins 1 and 2 and the disassembly of microtubules by the abnormal tau.* Proc Natl Acad Sci U S A, 1997. 94(1): p. 298-303.

4.   Grundke-Iqbal, I., et al., *Abnormal phosphorylation of the microtubule-associated protein tau (tau) in Alzheimer cytoskeletal pathology.* Proc Natl Acad Sci U S A, 1986. 83(13): p. 4913-7.

5.   Egger, G., et al., *Epigenetics in human disease and prospects for epigenetic therapy.* Nature, 2004. 429(6990): p. 457-63.

6.   Takai, D. and P.A. Jones, *Comprehensive analysis of CpG islands in human chromosomes 21 and 22.* Proc Natl Acad Sci U S A, 2002. 99(6): p. 3740-5.

7.   Polansky, J.K., et al., *Methylation matters: binding of Ets-1 to the demethylated Foxp3 gene contributes to the stabilization of Foxp3 expression in regulatory T cells.* J Mol Med (Berl), 2010. 88(10): p. 1029-40.

8.   Bird, A.P. and A.P. Wolffe, *Methylation-induced repression--belts, braces, and chromatin.* Cell, 1999. 99(5): p. 451-4.

9.   Colot, V. and J.L. Rossignol, *Eukaryotic DNA methylation as an evolutionary device.* Bioessays, 1999. 21(5): p. 402-11.

10.   Shibuya, K., S. Fukushima, and H. Takatsuji, *RNA-directed DNA methylation induces transcriptional activation in plants.* Proc Natl Acad Sci U S A, 2009. 106(5): p. 1660-5.

11.   Quina, A.S., M. Buschbeck, and L. Di Croce, *Chromatin structure and epigenetics.* Biochem Pharmacol, 2006. 72(11): p. 1563-9.

12.   Herman, J.G. and S.B. Baylin, *Gene silencing in cancer in association with promoter hypermethylation.* N Engl J Med, 2003. 349(21): p. 2042-54.

13.   Jones, P.A. and S.B. Baylin, *The fundamental role of epigenetic events in cancer.* Nat Rev Genet, 2002. 3(6): p. 415-28.

14.   Hanahan, D. and R.A. Weinberg, *The hallmarks of cancer.* Cell, 2000. 100(1): p. 57-70.

15.   Meichle, A., A. Philipp, and M. Eilers, *The functions of Myc proteins.* Biochim Biophys Acta, 1992. 1114(2-3): p. 129-46.

16.   Hanahan, D. and R.A. Weinberg, *Hallmarks of cancer: the next generation.* Cell, 2011. 144(5): p. 646-74.

17.   Zawia, N.H., D.K. Lahiri, and F. Cardozo-Pelaez, *Epigenetics, oxidative stress, and Alzheimer disease.* Free Radic Biol Med, 2009. 46(9): p. 1241-9.

18.   Gatz, M., et al., *Complete ascertainment of dementia in the Swedish Twin Registry: the HARMONY study.* Neurobiol Aging, 2005. 26(4): p. 439-47.

19.   Gatz, M., et al., *Heritability for Alzheimer's disease: the study of dementia in Swedish twins.* J Gerontol A Biol Sci Med Sci, 1997. 52(2): p. M117-25.

20.   Raiha, I., et al., *Alzheimer's disease in twins.* Biomed Pharmacother, 1997. 51(3): p. 101-4.

21.   Bassett, S.S., D. Avramopoulos, and D. Fallin, *Evidence for parent of origin effect in late-onset Alzheimer disease.* Am J Med Genet, 2002. 114(6): p. 679-86.

22.   Hall, J.G., *Genomic imprinting: review and relevance to human diseases.* Am J Hum Genet, 1990. 46(5): p. 857-73.

23.   Liu, L., Y. Li, and T.O. Tollefsbol, *Gene-environment interactions and epigenetic basis of human diseases.* Curr Issues Mol Biol, 2008. 10(1-2): p. 25-36.

24.   Mastroeni, D., et al., *Epigenetic differences in cortical neurons from a pair of monozygotic twins discordant for Alzheimer's disease.* PLoS One, 2009. 4(8): p. e6617.

25.   Cacabelos, R., *Pharmacogenomics in Alzheimer's disease.* Methods Mol Biol, 2008. 448: p. 213-357.

26.   Chen, K.L., et al., *The epigenetic effects of amyloid-beta(1-40) on global DNA and neprilysin genes in murine cerebral endothelial cells.* Biochem Biophys Res Commun, 2009. 378(1): p. 57-61.

27.   Russo, R., et al., *Neprylisin decreases uniformly in Alzheimer's disease and in normal aging.* FEBS Lett, 2005. 579(27): p. 6027-30.

28.   Antonell, A., et al., *A preliminary study of the whole-genome expression profile of sporadic and monogenic early-onset Alzheimer's disease.* Neurobiol Aging, 2013. 34(7): p. 1772-8.

29.   Martinez, T. and A. Pascual, *Gene expression profile in beta-amyloid-treated SH-SY5Y neuroblastoma cells.* Brain Res Bull, 2007. 72(4-6): p. 225-31.

30.   Kong, L.N., et al., *Gene expression profile of amyloid beta protein-injected mouse model for Alzheimer disease.* Acta Pharmacol Sin, 2005. 26(6): p. 666-72.

31.   Darst, R.P., et al., *Bisulfite sequencing of DNA.* Curr Protoc Mol Biol, 2010. Chapter 7: p. Unit 7 9 1-17.

32.   Raizis, A.M., F. Schmitt, and J.P. Jost, *A bisulfite method of 5-methylcytosine mapping that minimizes template degradation.* Anal Biochem, 1995. 226(1): p. 161-6.

33.   Licchesi, J.D. and J.G. Herman, *Methylation-specific PCR.* Methods Mol Biol, 2009. 507: p. 305-23.

34. Melnikov, A.A., et al., *MSRE-PCR for analysis of gene-specific DNA methylation.* Nucleic Acids Res, 2005. 33(10): p. e93.

35. Figueroa, M.E., A. Melnick, and J.M. Greally, *Genome-wide determination of DNA methylation by Hpa II tiny fragment enrichment by ligation-mediated PCR (HELP) for the study of acute leukemias.* Methods Mol Biol, 2009. 538: p. 395-407.

36. Oda, M., et al., *High-resolution genome-wide cytosine methylation profiling with simultaneous copy number analysis and optimization for limited cell numbers.* Nucleic Acids Res, 2009. 37(12): p. 3829-39.

37. Khulan, B., et al., *Comparative isoschizomer profiling of cytosine methylation: the HELP assay.* Genome Res, 2006. 16(8): p. 1046-55.

38. Palmke, N., D. Santacruz, and J. Walter, *Comprehensive analysis of DNA-methylation in mammalian tissues using MeDIP-chip.* Methods, 2011. 53(2): p. 175-84.

39. Curran, D.R., et al., *Mechanism of eosinophil induced signaling in cholinergic IMR-32 cells.* Am J Physiol Lung Cell Mol Physiol, 2005. 288(2): p. L326-32.

40. Asami-Odaka, A., et al., *Long amyloid beta-protein secreted from wild-type human neuroblastoma IMR-32 cells.* Biochemistry, 1995. 34(32): p. 10272-8.

41. Oakley, H., et al., *Intraneuronal beta-amyloid aggregates, neurodegeneration, and neuron loss in transgenic mice with five familial Alzheimer's disease mutations: potential factors in amyloid plaque formation.* J Neurosci, 2006. 26(40): p. 10129-40.

42. Taher, N., et al., *Amyloid-beta Alters the DNA Methylation Status of Cell-fate Genes in an Alzheimer's Disease Model.* J Alzheimers Dis, 2014. 38(4): p. 831-44.

43. Kulaeva, O.I., et al., *Distant activation of transcription: mechanisms of enhancer action.* Mol Cell Biol, 2012. 32(24): p. 4892-7.

44. Marsman, J. and J.A. Horsfield, *Long distance relationships: enhancer-promoter communication and dynamic gene transcription.* Biochim Biophys Acta, 2012. 1819(11-12): p. 1217-27.

45. Cobos, I., U. Borello, and J.L. Rubenstein, *Dlx transcription factors promote migration through repression of axon and dendrite growth.* Neuron, 2007. 54(6): p. 873-88.

46. Chen, L., et al., *VHL regulates the effects of miR-23b on glioma survival and invasion via suppression of HIF-1alpha/VEGF and beta-catenin/Tcf-4 signaling.* Neuro Oncol, 2012. 14(8): p. 1026-36.

47. Lee, K. and K. Rhee, *PLK1 phosphorylation of pericentrin initiates centrosome maturation at the onset of mitosis.* J Cell Biol, 2011. 195(7): p. 1093-101.

48. Wang, Y., et al., *Promoter hijack reveals pericentrin functions in mitosis and the DNA damage response.* Cell Cycle, 2013. 12(4): p. 635-46.